Int. J. Electrochem. Sci., 12 **(2017)** 6292 – 6303, doi: 10.20964/2017.07.75

International Journal of
ELECTROCHEMICAL
SCIENCE
www.electrochemsci.org

Solvothermal Synthesized γ-Fe_2O_3/graphite Composite for Supercapacitor

Miao Wang[1], *Suzhen Cheng*[1] , *Guoju Dang*[1,3], *Fanqi Min*[1,3],*Haiyan Li*[1], *Quansheng Zhang*[1,*], *Jingying Xie*[2,3,*]

[1] Department of Chemical Engineering, Shanghai Institute of Technology, Shanghai 200235, China
[2] Shanghai Institute of Space Power Sources, Shanghai 200245, China
[3] Shanghai Power & Energy Storage Battery System Engineering Tech. Co. Ltd., Shanghai 200240, China
[*]E-mail: zhangquansheng@sit.edu.cn, jyxie@mail.sim.ac.cn

Received: 4 April 2017 / *Accepted:* 17 May 2017 / *Published:* 12 June 2017

This article described a facile solvothermal synthesis method for γ-Fe_2O_3/graphite composite preparation with liquid phase exfoliated graphite (Gp), Fe^{3+} ($FeCl_3$•$6H_2O$), and NaOH precipitants. The γ-Fe_2O_3/graphite composite was characterized by X-ray powder diffraction (XRD), Scanning and transmission electron microscopy (SEM and TEM), Energy dispersive spectroscopy (EDS) and Thermogravimetric (TG) analysis. The electrochemical properties of γ-Fe_2O_3/graphite composite as electrode materials for supercapacitor were investigated by cyclic voltammetry and galvanostatic charge-discharge tests. The results showed that specific capacity of γ-Fe_2O_3/graphite composite is 520 F g^{-1} at 3A g^{-1} in 1M KOH aqueous electrolyte and capacity retention is 91.3% after 1000 charge-discharge cycles.

Keywords: γ-Fe_2O_3, Graphite, Solvothermal synthesis, Supercapacitor

1. INTRODUCTION

In recent years, supercapacitors are regarded as one of the newest innovative device for electrochemical energy storage, which have attracted much attention for their high energy and power density, rapid charge-discharge capability, excellent reversibility and long cyclic life [1-7]. Great efforts have been dedicated to the construction of supercapacitor electrode using various metal oxides and carbon-based materials. The capacity of supercapacitor can be improved by metal oxides that appended to active materials due to pseudo electrical property of metal oxides, such as RuO_2, Fe_2O_3, NiO, Co_3O_4, MnO_2, etc [8-13].

Iron oxides (FeO_x) are admitted as promising anode materials applied to supercapacitors, because of their low cost, abundant storage on earth, low toxicity, environmental friendliness [14-19]. However, their poor electrical conductivities are detrimental to electrode applications [20-25]. To enhance the capacitive performance, the intensive research efforts are being made to combine FeO_x with high-conductive materials, such as carbon nanotubes [26], activated carbon [27], carbon fiber, graphene [28-31]. Those high-conductive materials have been adopted as an enhancing reagent for the charge transport involved in the capacitance generation process of FeO_x. Hsuan-Ching Chen reported that potentiostatic deposited γ-Fe_2O_3/graphene nanocomposite with 5 nm γ-Fe_2O_3 nanocrystals on porous graphene film exhibit a specific capacitance of 224 F g^{-1} in 1 M Na_2SO_3 at 25mV s^{-1} [32]. Ying Li proposed the Fe_2O_3 loaded activated carbon prepared by solvothermal synthesis with NaOH/$FeCl_3$ molar ratio being 1.5 that shown excellent rate capability with specific capacitance of 215 F g^{-1} at 1 A g^{-1}[33]. The general capacitive properties of FeO_x had be improved, but the existed issues were still remained, such as insufficient high rate capability and cycling stability, which limited the further development of FeO_x as an effective anode material in supercapacitors [32-34].

In this paper, we report a one-step solvothermal process to synthesize the γ-Fe_2O_3/graphite nanocomposite using Fe^{3+} and liquid-phase exfoliated graphite sheets (Gp) as raw materials, and the γ-Fe_2O_3/graphite as the electrode active material of supercapacitor was studied.

2. EXPERIMENTAL

2.1. Synthesis of γ-Fe_2O_3/graphite composite materials

0.54g $FeCl_3·6H_2O$ was dissolved with 50 mL N-methylpyrrolidone (NMP), followed by addition of 7 mL liquid exfoliated graphite dispersion, which was prepared by 20 g graphite mixed with 1 L NMP under ultrasonic bath for 20 h. After that, solution of 0.4g NaOH in 25 mL NMP was dropped to the above mentionedmixture. accompanied with vigorous stirring for 1 h. The final mixture was sealed in a Teflon-lined stainless steel autoclave and maintained at 200 °C for 18 h, then cool down to room temperature naturally. The black product was isolated by centrifugation, repeatedly washed with distilled water and absolute ethanol respectively, and dried at 60 °C to gain the γ-Fe_2O_3/graphite (γ-Fe_2O_3/Gp) composite materials. And the pure γ-Fe_2O_3 material was gained without added the exfoliated graphite dispersion.

2.2 Electrode preparation

The electrode material composition was of γ-Fe_2O_3/Gp, Super P and Polytetrafluoroethylene (PTFE) in weight ratio of 8:1:1. NMP was used to make the composited electrode material as electrode slurry under high speed stirring. The test electrode was fabricated by coat the electrode slurry into Ni foam dried under vacuum at 60 °C for 12 h.

2.3 Characterization techniques

Scanning electron microscopy (SEM) images of the as-synthesized samples were obtained by the S-3400N field emission scanning electron microscope operated at 15 Kv. The microstructure of γ-Fe_2O_3/Gp composite was observed with analytical transmission electron microscopy (TEM; Tecnai-G2-F30, 200 kV). X-ray diffraction (XRD) was performed with the X'Pert PW3040/60 X-ray diffraction with Cu Kα radiation (40 kV, 40 mA) to identify the crystal structure. The oxidation states of Fe were characterized with an energy-dispersive X-ray Photoelectron spectrometer (XPS). Raman spectrometer (T64000 HORIBA Jobin Yvon) using a 50 mW and 514.5 nm wavelength Ar green laser was applied to identify graphite in the prepared γ-Fe_2O_3/Gp. Thermogravimetric analysis (TGA) data was collected on a thermal analysis instrument (NETZSCH, STA 449F3) with a heating rate of 10 °C/min under air flow.

Cyclic voltammetry (CV) was measured by a CHI760D electrochemical workstation (Shanghai Chenhua Co. Ltd. China). Galavanostatic charge/discharge measurement was performed too. All electrochemical experiments were carried out in a three-electrode system with a reference electrode in 1M KOH aqueous electrolyte at room temperature.

3. RESULTS AND DISCUSSION

3.1. Characterization of γ-Fe_2O_3/Gp composite

The SEM images of the γ-Fe_2O_3 and the γ-Fe_2O_3/Gp composite prepared by solvothermal synthesized were shown in Fig.1. As shown in Fig. 1a), the morphology of pure γ-Fe_2O_3 appeared as a pile of irregular and agglomerate mirco- and nano-particles. With regard to γ-Fe_2O_3/Gp composite, the γ-Fe_2O_3 nanoparticles were more uniformly distributed on the surface of exfoliated graphite and the specific three dimensional porous structures can be seen in Fig. 1b).

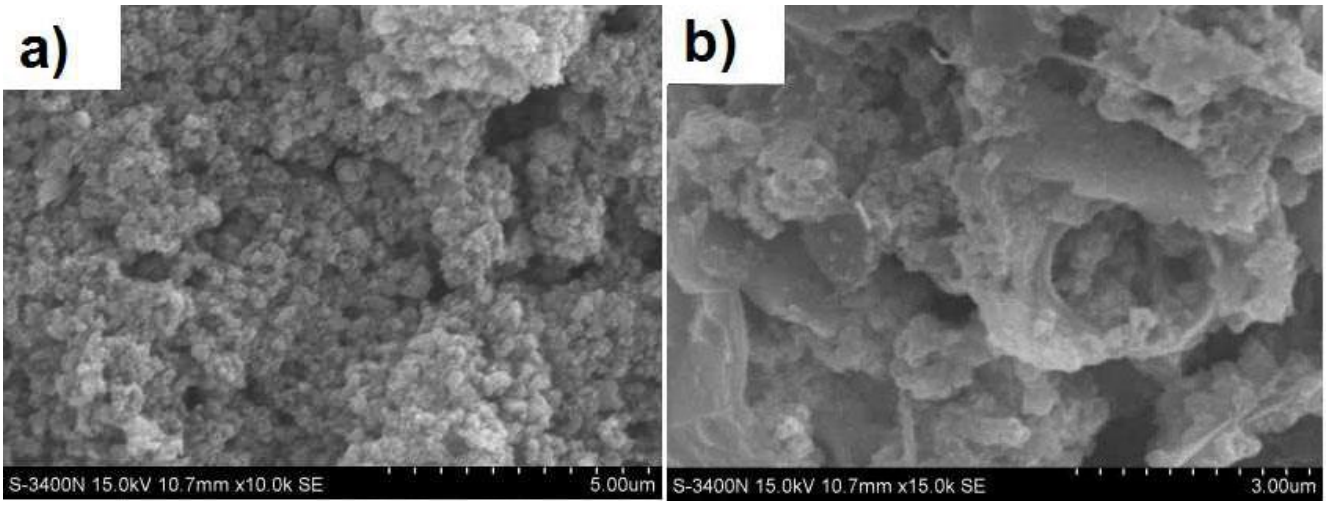

Figure 1. SEM images of a) γ-Fe_2O_3, b) γ-Fe_2O_3/Gp composite

In the meantime, the specific three dimensional structures can be not only efficacious restrained the reunion phenomenon of γ-Fe_2O_3, which increased dispersion consistency of γ-Fe_2O_3 on the surface of exfoliated graphite, but also observably increased the ion's transport/transfer performance between electrode interface and electrolyte during the charge-discharge cycle process, which might be increased the contact area between γ-Fe_2O_3 and exfoliated graphite and electrolyte, resulted in the promotion of energy density and power density [32].

Fig. 2 shows the N_2 adsorption-desorption isotherms, the BET specific surface area and BJH pore parameters of the γ-Fe_2O_3/Gp composite. As shown in insets of Fig. 2, the BET specific surface area (S_{BET}) of the γ-Fe_2O_3/Gp composite is 78.7 $m^2 g^{-1}$, and the BJH desorption pore volumes (V*pore*) of the γ-Fe_2O_3/Gp composite is 0.46 $cm^3 g^{-1}$, the most probable pore size is 6.2 nm, that due to the specific three dimensional structures of the γ-Fe_2O_3/Gp composite. For capacitive applications, high V*pore* and S_{BET} provide not only surface reaction sites but also sufficient buffer space to alleviate the volume expansion of γ-Fe_2O_3 during charge-discharge cycling, and are therefore favorable for the electrochemical properties [33]. These BET analyses can partially explain the superior capacitive performance of γ-Fe_2O_3/Gp composite.

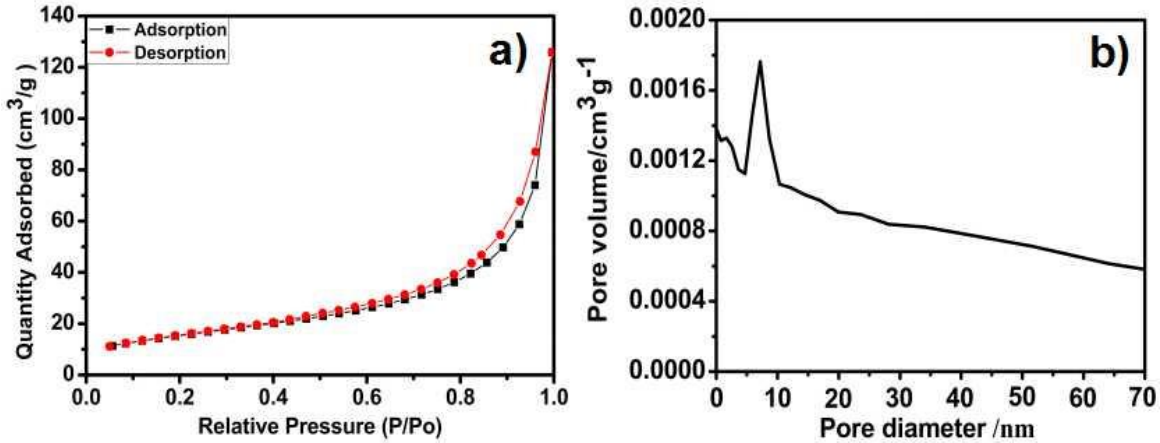

Figure 2. a) N_2 adsorption-desorption isotherm of the γ-Fe_2O_3/Gp; b) BJH pore size distribution of the γ-Fe_2O_3/Gp

The detailed morphological and crystallographic structures of the γ-Fe_2O_3/Gp composite were investigated by TEM and HRTEM. As shown in Fig. 3a), a large amount of the γ-Fe_2O_3 nanoparticles were uniformly distribute on the surface of exfoliated graphite nano sheets after the solvohermal treatments. The average size of γ-Fe_2O_3/Gp was about 20 nm. The HRTEM image in Fig. 3b) shows that the interplanar distance between the lattice fringes ware 0.25 nm, corresponding to the characteristic interlayer distances in the (311) direction for γ-Fe_2O_3, and the interplanar distance of the (002) direction was 0.34 nm for exfoliated graphite [32]. The results show that the prepared γ-Fe_2O_3/Gp composite is pure nano-scale particles without reuniting.

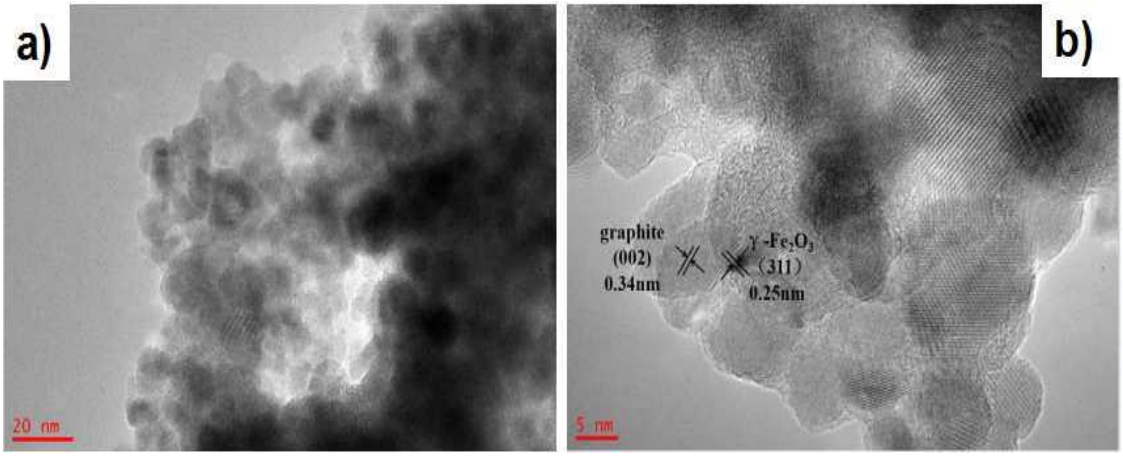

Figure 3. a) Low and b) high magnification TEM images taken of γ-Fe_2O_3/Gp composite

The crystallographic structure of the γ-Fe_2O_3, the Gp and the γ-Fe_2O_3/Gp composite material were evaluated by X-ray diffraction, as shown in Fig. 4. Compared with the XRD figures of γ-Fe_2O_3 and γ-Fe_2O_3/Gp and Gp, we can know that the diffraction patterns of γ-Fe_2O_3/Gp were included the all characteristic peaks of γ-Fe_2O_3 and Gp. The broad characteristic diffraction peak at about 27° was found in the diffraction pattern of Gp, and this obvious diffraction peak was appeared in the XRD patterns of γ-Fe_2O_3/Gp composite alike. The diffraction peaks of γ-Fe_2O_3/Gp, including (220), (311), (222), (400), (511) and (440) at the 2θ values of 30.2°, 35.6°, 37.2°, 43.3°, 57.3° and 62.8°, respectively, are matched with the characteristic diffraction peaks for γ-Fe_2O_3 (JCPDS#39-1346) [32]. It is well known that the X-ray diffraction patterns of Fe_3O_4 and γ-Fe_2O_3 are quite similar [32], so the further characterizations should be carried out to differentiate the two.

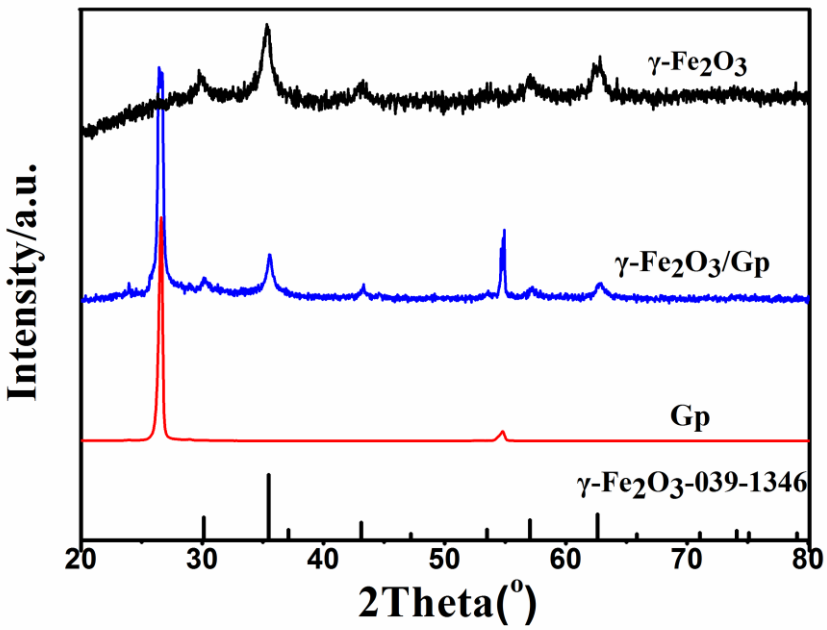

Figure 4. The XRD images of γ-Fe_2O_3 and γ-Fe_2O_3/Gp composite

The XPS analysis was carried out, which is very sensitive to Fe^{2+} and Fe^{3+} cations [38]. Fig. 5 shows the XPS spectra of Fe 2p of the γ-Fe_2O_3/Gp composite material. The characteristic binding energy peaks were located at 724.6 and 710.8 eV assigned to Fe $2p_{1/2}$ and Fe $2p_{3/2}$. It's more important that the satellite peak at 718.8 eV was considered as the characteristic peak of γ-Fe_2O_3, and is absent in the XPS spectrum of Fe_3O_4 [23, 37].

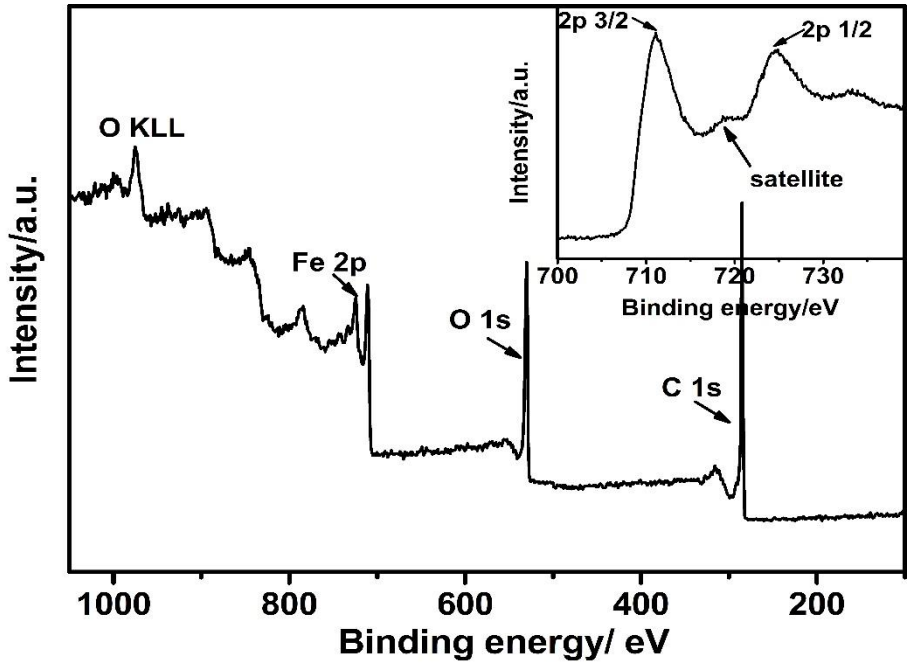

Figure 5. XPS spectrum of the γ-Fe_2O_3/Gp and Fe2p spectra of γ-Fe_2O_3/Gp (inset)

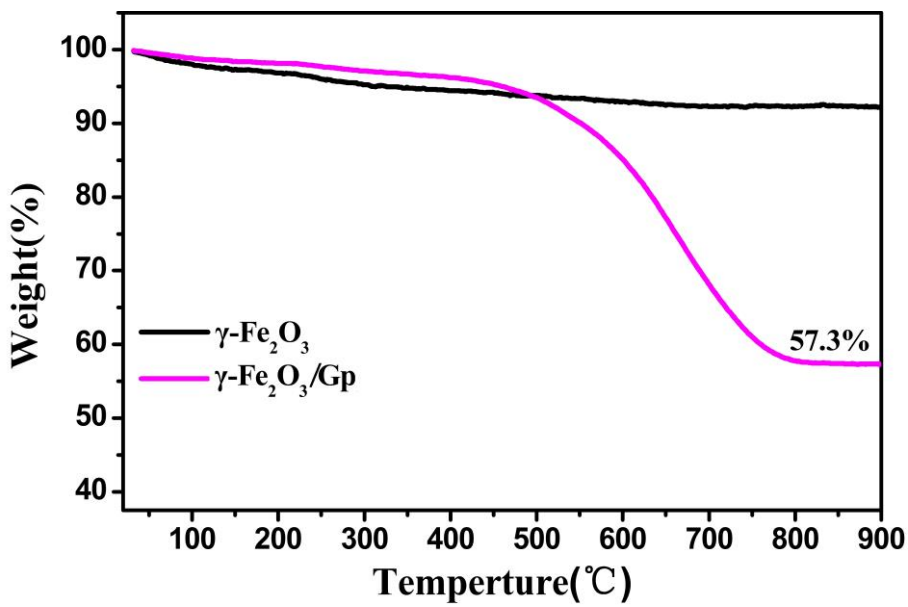

Figure 6. TG images of γ-Fe_2O_3 and γ-Fe_2O_3/Gp samples in nitrogen atmospheres

To further confirm that our product is γ-Fe_2O_3, but not Fe_3O_4, TG analysis of the γ-Fe_2O_3/Gp and γ-Fe_2O_3 were conducted. For Fe_3O_4, it will be oxidized to Fe_2O_3 at high temperatures and thus a weight pickup occurs at high temperatures [23]. From Fig. 6, we can find that the weight gain phenomena were not existed in TG analyses of γ-Fe_2O_3 and γ-Fe_2O_3/Gp. The γ-Fe_2O_3/Gp composite was experienced a significant weight loss from 450 to 750 °C, which was caused by the oxidation of graphite formed carbon dioxide. As for the γ-Fe_2O_3/Gp composite, the remaining weight percentage remained constant after 750 °C and no weight pickup can be observed up to 900 °C. And the γ-Fe_2O_3 was without weight pickup almostly. This TG analysis further confirm again the formation of γ-Fe_2O_3/Gp composite as the product of the deposition, without Fe_3O_4.

To prove that our material is Gp and γ-Fe_2O_3, Fig. 7 exhibits the Raman spectra of the γ-Fe_2O_3/Gp composite. The three prominent peaks of the exfoliated graphite were displayed, including a G band at about 1577 cm^{-1}, a second-order two-phonon-mode 2D band at about 2700 cm^{-1}, and a disorder-related D peak at about 1347 cm^{-1} [39]. According to the test results, there could be found that the prominent peak of the γ-Fe_2O_3 at about 1430 cm^{-1}, and a A_{1g} band of the Fe_2O_3 at about 218 cm^{-1}, and a E_{1g} band of the Fe_2O_3 at about 382 cm^{-1}, which indicated that the composite is composed of graphite and γ-Fe_2O_3.

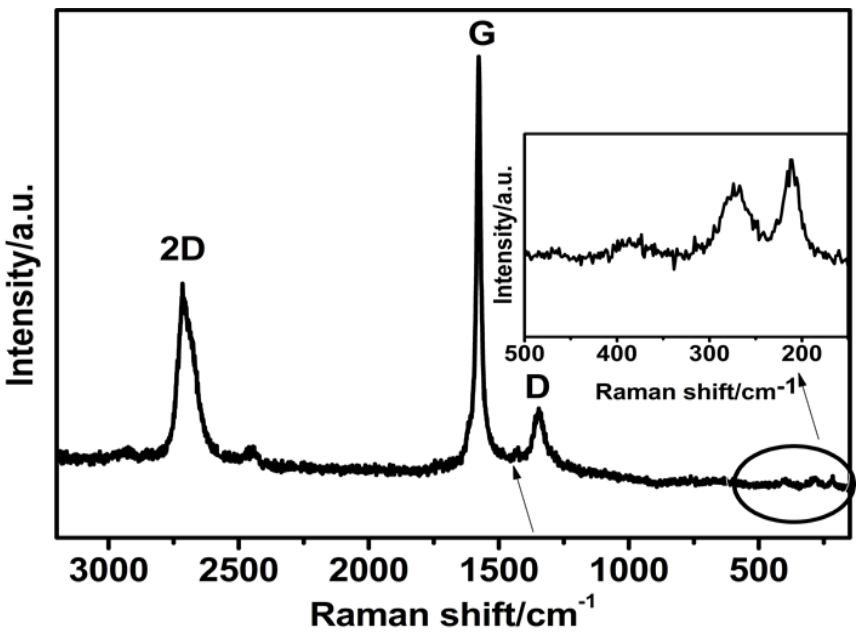

Figure 7. Raman spectra of γ-Fe_2O_3/Gp composite

3.2. Capacitive performances of γ-Fe_2O_3/Gp composite

The electrochemical performances of the γ-Fe_2O_3 and the γ-Fe_2O_3/Gp composite were characterized by cyclic voltammetry (CV) and galvanostatic charge-discharge (GCD) test. Fig. 8a) shows the test results of CV curves of the γ-Fe_2O_3 and the γ-Fe_2O_3/Gp electrodes in 1M KOH. In Fig.8a) at 5 mV s^{-1} scan rate within a potential window from -1.2 to 0 V (vs. Hg/HgO). The CV curves

of the γ-Fe_2O_3/Gp electrode was provided with nearly symmetrical with redox peaks, it is commendable evident that the samples were demonstrated possess pseudocapacitive properties. Moreover, on the basis of the CV curve, the current density and integral area of the γ-Fe_2O_3/Gp electrode were much larger than the γ-Fe_2O_3 electrode, the capacity of the γ-Fe_2O_3 electrode is 140 F g^{-1}, the capacity of the γ-Fe_2O_3/Gp electrode is 423 F g^{-1}, which showed the γ-Fe_2O_3/Gp own the higher capacitance. The CV curves of the γ-Fe_2O_3/Gp electrode at a range of scan rates from 5 to 100 mV s^{-1} were shown in Fig. 8b), which revealed its good electrochemical reversibility and high power characteristics.

The liquid phase exfoliated graphite (Gp) with layered structure show high surface area, high conductivity. That the addition of Gp on electrochemical property of γ-Fe_2O_3 change is very outstanding. The main reason is as follows: γ-Fe_2O_3 suffers from aggregation after reaction, poor capacity retention and low electronic conductivity. The loading of γ-Fe_2O_3 on Gp can not only solve these problems but also minimize the aggregation or restacking of Gp and enhance the properties of Gp.

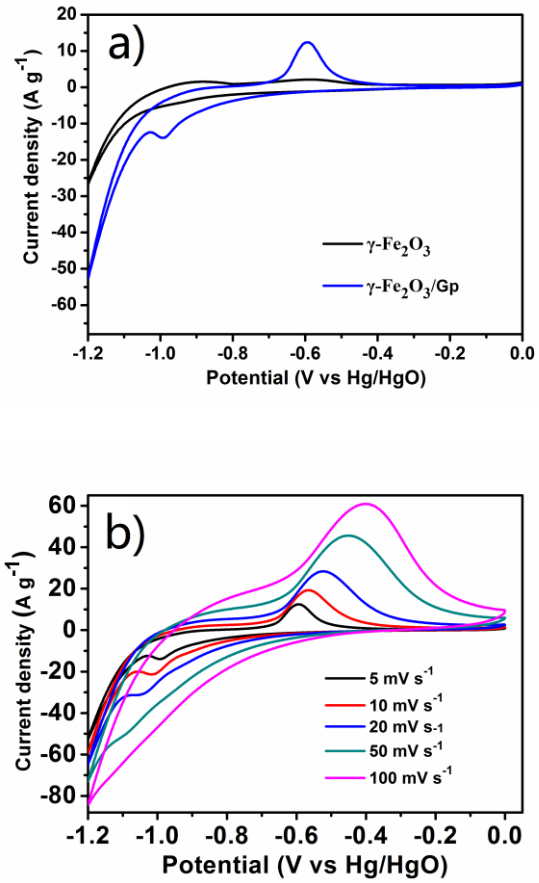

Figure 8. a) CV curves of the γ-Fe_2O_3/Gp electrode at the scan rate of 5mV s^{-1} within a potential window from -1.2 to 0 V; b) The CV curves of the γ-Fe_2O_3/Gp electrode at a range of scan rates from 5 to 100 mV s^{-1}

Fig. 9a) shows the galvanostatic charge–discharge curves and rate performance of the γ-Fe_2O_3/Gp composite at current densities from 3 to 10A g^{-1}. The γ-Fe_2O_3/Gp composite was presented two different variation trends during the charge steps. As the potential is lower than 0.75V, the potential varies linearly with time indicating the pure double-layer capacitance behavior at the electrode–electrolyte interface. The potential nonlinear after 0.75V is due to the typical pseudocapacitance of γ-Fe_2O_3/Gp.

The specific capacitance C_s (F g^{-1}) has been calculated based on the following equation:

C_s (F g^{-1}) = $I\Delta t/m\Delta V$

where I (mA) is the current used for charge–discharge, Δt (s) is the time rate for the discharge cycle, *m* (mg) is the weight of the active material, and Δ*V* (V) is the potential drop during discharge.

The specific capacitances of the γ-Fe_2O_3 and the γ-Fe_2O_3/Gp materials at different charge and discharge current density were calculated and shown in Fig. 9b). Therefore, the specific capacitance values of the γ-Fe_2O_3/Gp composite are 520、418、390、360、320 and 238 F g^{-1} corresponding to current densities of 3、4、5、6、7 and 10 A g^{-1} respectively. Obviously, based on the test results, the γ-Fe_2O_3/Gp composite electrode all have higher capacity than the γ-Fe_2O_3 electrode. It is in agreement with CV profiles.

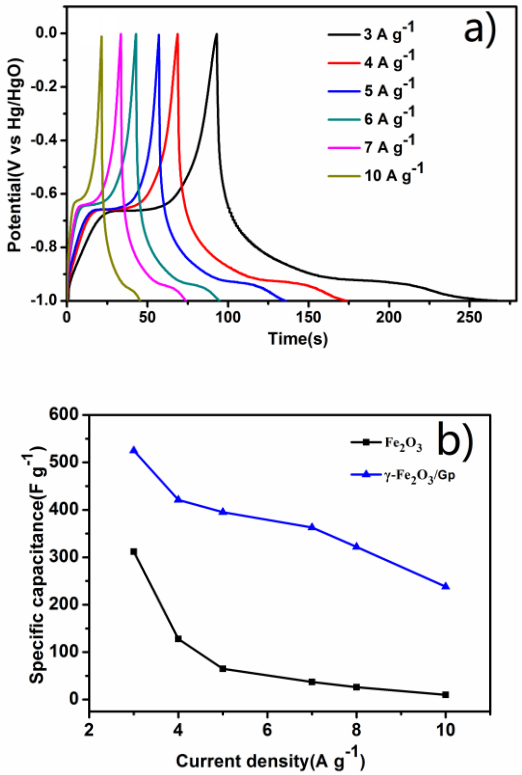

Figure 9. a) The galvanostatic charge-discharge(GCD) curves of γ-Fe_2O_3/Gp at current densities from 3 to 10 A g^{-1}; b) The specific capacitance of the γ-Fe_2O_3 and γ-Fe_2O_3/Gp composites at different current densities (3, 4, 5, 6, 7, 10A g^{-1})

Long term cycling stability is a defining key parameter for the practical application for supercapacitors, and the variety of capacitance retention as a function of cycle number at 3 A g^{-1} was

known in Fig. 10. The γ-Fe_2O_3/Gp composite could be retained about 91.3% of its initial capacitance value after 1000 cycles, while the capacitance of pure γ-Fe_2O_3 had faded to 74.3% its initial value after 1000 cycles. The γ-Fe_2O_3/Gp composite shows the better cycling stability due to the exfoliated graphite substrate in composite electrode.

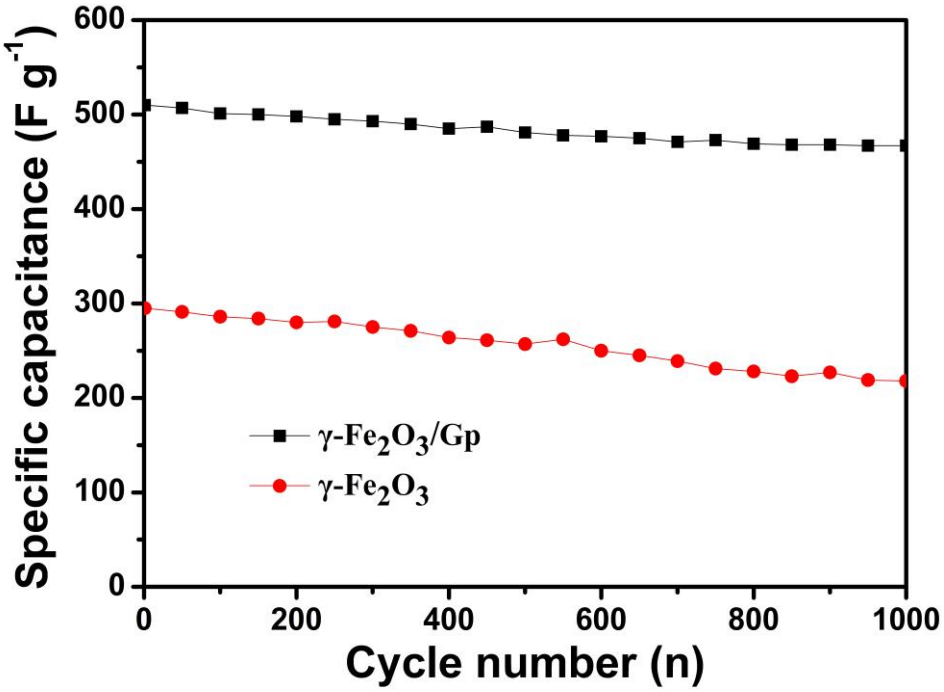

Figure 10. Cycling performance of γ-Fe_2O_3 and γ-Fe_2O_3/Gp at a current density of 3 A g^{-1}

The comparison of the specific capacitances performance of the γ-Fe_2O_3/Gp electrode materials with other electrode materials reported in literatures for the application of supercapacitor was shown in Table 1. The results in this table showed that γ-Fe_2O_3/Gp electrode exhibits higher capacity than other electrodes, indicating γ-Fe_2O_3/Gp material synthesized by solvothermal method in this work own very good the electrochemical performance and capacity.

Table 1. A summary of the electrode materials and their corresponding specific capacitances

Composition	Specific capacitance and current density	Ref.
Fe_2O_3/graphene sheets synthesized by chemical precipitation	151.8 F g^{-1} with 1A g^{-1} 120 F g^{-1} with 6A g^{-1}	[40]
Fe_2O_3/graphene sheets synthesized by hydrothermal method	181 F g^{-1} with 3A g^{-1} 69 F g^{-1} with 6A g^{-1}	[41]
Fe_2O_3/graphene sheets synthesized by hydrothermal method	226 F g^{-1} with 1A g^{-1}	[42]
γ-Fe_2O_3/Gp solvothermal synthesized in this work	520 F g^{-1} with 3A g^{-1} 360 F g^{-1} with 6A g^{-1}	This work

4. CONCLUSIONS

In summary, the γ-Fe_2O_3/Gp composite for supercapacitors were successfully prepared by solvothermal method. The γ-Fe_2O_3/Gp composite exhibited a higher specific capacitance and the higher cycling stability compared to the pure γ-Fe_2O_3 composite.

The γ-Fe_2O_3/Gp composite achieved specific capacitance of 520 F g^{-1} at 3 A g^{-1} in 1M Na_2SO_4 electrolyte and also a high capacitance retention of 91.3% at 3 A g^{-1} after 1000 times charging/discharging cycles. As a result, the γ-Fe_2O_3/Gp composite synthesized by this strategy are expected to be further extended to other energy storage device applications. It is believed that this study would open one way for other metal oxide nanomaterials with excellent electrochemical performances.

ACKNOWLEDGEMENTS
This work was supported by the National Natural Science Foundation of China (No. 21373137), National 863 Program (No. 2014AA052202), Shanghai Science and Technology Development Funds (No. 13DZ2280200 & No. 15DZ2282000).

References

1. L. Wang, H. M. Ji, S. S. Wang, L. J. Kong, X. F. Jiang, G.Yang, *RSC.*, 5 (2013) 3793.
2. B. E. Conway, *J. Electrochem. Soc.*,138 (1991) 1539.
3. M. Winter and R. J. Brodd, *Chem. Rev.*, 104 (2004) 4245.
4. B. G. Choi, S. J. Chang, H. W. Kang, C. P. Park, H. J. Kim, W. H. Hong, S. Lee and Y. S. Huh, *Nanoscale.*, 4 (2012) 4983.
5. F. L. Zheng, G. R. Li, Y. N. Ou, Z. L. Wang, C. Y. Su and Y. X. Tong, *Chem. Commun.*, 46 (2010) 5021.
6. J. Bae, M. K. Song, Y. J. Park, J. M. Kim, M. Liu and Z. Wang, *Angew. Chem. Int. Ed.*, 50 (2011) 1683.
7. S. L. Xiong, C. Z. Yuan, X. G. Zhang, B. J. Xi and Y. T. Qian, *Chem. Eur. J.*, 15 (2009) 5320.
8. S. Z. Cheng, S. Li, J. Xia, T. H. Lei, Q. S. Zhang, J. Y. Xie. *RSC Advances. J. Name.*, 00 (2013) 1.
9. Z. S. Wu, D. W. Wang, W. Ren, J. Zhao, G. Zhou, F. Li and H. M. Cheng, *Adv. Funct. Mater.*, 20 (2010) 3595.
10. J. Mu, B. Chen, Z. Guo, M. Zhang, Z. Zhang, P. Zhang, C. Shao and Y. Liu, *Nanoscale.*, 3 (2011) 5034.
11. H. Wang, H. Yi, X. Chen and X. Wang, *Electrochim. Acta.*, 105 (2013) 353.
12. W. Zhang, F. Liu, Q. Li, Q. Shou, J. Cheng, L. Zhang, B. J. Nelson and X. Zhang, *Phys. Chem. Chem. Phys.*, 14 (2012) 16331.
13. Y. Q. Zhao, D. D. Zhao, P. Y. Tang, Y. M. Wang, C. L. Xu and H. L. Li, *Mater. Lett.*, 76 (2012) 127.
14. W. Jin, G. Cao and J. Sun, *J. Power Sources.*, 175 (2008) 686.
15. H. Y. Quan, B. C. Cheng, Y. H. Xiao and S. J. Lei, *Chemical Engineering Journal.*, 286 (2016) 165.
16. T. Brousse and D. Belanger. *Electrochem. Solid-State Lett.*, 6 (2003) A244.
17. T. Cottineau, M. Toupin, T. Delahaye, T. Brousse and D. Belanger, *Appl. Phys. Mater. Sci. Process.*, 82 (2006) 599.
18. M. Wu and R. Lee, *J. Electrochem. Soc.*, 156 (2009) A737.

19. Q. Qu, S. Yang and X. Feng, *Adv. Mater.*, 23 (2011) 5574.
20. J. Chen, K. Huang and S. Liu, *Electrochim. Acta.*, 55 (2009) 1.
21. M. Wu, R. Lee, J. Jow, W. Yang, C. Hsieh and B. Weng, *Electrochem. Solid-State Lett.*, 12 (2009) A1.
22. K. Xie, J. Li, Y. Lai, W. Lu, Z. Zhang, Y. Liu, L. Zhou and H. Huang, *Electrochem. Commun.*, 13 (2011) 657.
23. N. Nagarajan and I. Zhitomirsky, *J Appl. Electrochem.*, 36 (2006) 1399.
24. S. Pang, W. Khoh and S. Chin, *J. Mater. Sci.*, 45 (2012) 5598.
25. K. Chumg, K. Kim, S. Han and H. Lee, *Electrochem. Solid-State Lett.*, 8 (2005) A259.
26. Y. Kim and S. Park, *Curr. Appl. Phys.*, 11(2011) 462.
27. M. B. Sassin, A. N. Mansour, K. A. Pettigrew, D. R. Rolison and J. W. Long, *ACS Nano.*, 4 (2010) 4505.
28. W. Shi, J. Zhu, D. H. Sim, Y. Y. Tay, Z. Lu, X. Zhang, Y. Sharma, M. Srinivasan, H. Zhang, H. H. Hng and Q. Yan, *J. Mater. Chem.*, 21 (2011) 3422.
29. Z. X. Song, W. Liu, W. S. Wei, C. Z. Quan, N. X. Sun, Q. Zhou, G. C. Liu and X. Q. Wen, *Journal of Alloys and Compounds.*, 685 (2016) 355.
30. Y. Gao, D. L. Wu, T. Wang, D. Z. Jia, W. Xia, Y. Lv, Y. L. Cao, Y. Y. Tan and P. G. Liu, *Electrochimica Acta.*, 191 (2016) 275.
31. C. J. Zhao, X. X. Shao, Y. X. Zhang and X. Z. Qian, *ACS Appl. Mater. Interfaces.*, 8 (2016) 30133.
32. H. C. Chen, C. C. Wang and S. Y. Lu, *J. Mater. Chem. A.*, 2 (2014) 16955.
33. Y. Li, L. T. Kang, G. L. Bai, P. Y. Li, J. C. Deng, X. G. Liu, Y. Z. Yang, F. Gao, W. Liang, *Electrochimica Acta.*, 134 (2014) 67.
34. M. B. Sassin, A. N. Mansour, K. A. Pettigrew, D. R. Rolison and J. W. Long, *ACS Nano.*, 4 (2010) 4505.
35. D. Wang, Y. Li, Q. Wang and T. Wang, *J. Solid State Electrochem.*, 16 (2012) 2095.
36. M. Zhang, E. Z. Liu, T. T. Cao, H. Y. Wang, C. S. Shi, J. J. Li, C. N. He, F. He, L.Y. Ma and N. Q. Zhao, *J. Mater. Chem. A.*, 00 (2017) 1.
37. T. Yamashita and P. Hayes, *Appl. Surf. Sci.*, 254 (2008) 2441.
38. B. Li, H. Q. Cao, J. Shao, M. Z. Qu and J. H. Warner, *J. Mater. Chem.*, 21 (2011) 5069.
39. A. Rauf, S. S. A. Shah, S. A. Rakha, *Int. J. Mod. Phys. B.*, 31 (2017) 1750118.
40. D. W. Wang, Y. Q. Li, Q. H. Wang, T. M. Wang, *J. Solid State Electrochem.*, 16 (2011) 2095.
41. K. K. Lee, S. Deng, H. M. Fan, S. Mhaisalkar, H. R. Tan, E. S. Tok, K. P. Loh, W. S. Chin, C. H. Sow, *Nanoscale.*, 4 (2012) 2958.
42. Z. Wang, C. Y. Ma, H. L. Wang, Z. H. Liu, Z. H. Hao, *Alloys Compd.*, 552 (2013) 486.